Comparison of Nanofiltration with Reverse Osmosis in Reclaiming Tertiary Treated Municipal Wastewater for Irrigation Purposes

MhdAmmar Hafiz[1], Alaa H. Hawari[1,*], Radwan Alfahel[1], Mohammad K. Hassan[2], Ali Altaee[3]

[1] Department of Civil and Architectural Engineering, Qatar University, Doha P.O. Box 2713, Qatar;
mh1201889@qu.edu.qa (M.H.); ra1404482@qu.edu.qa (R.A.)
[2] Center for Advanced Materials, Qatar University, Doha P.O. Box 2713, Qatar; mohamed.hassan@qu.edu.qa
[3] School of Civil and Environmental Engineering, University of Technology in Sydney, 15 Broadway,
Ultimo, NSW 2007, Australia; Ali.Altaee@uts.edu.au
***** Correspondence: a.hawari@qu.edu.qa; Tel.: +974-4403-4184

[*]Corresponding author: Dr. Alaa H. Hawari, Department of Civil and Architectural Engineering, College of Engineering, Qatar University, 2713 Doha, Qatar.
Email: a.hawari@qu.edu.qa

Abstract

This study investigates the performance of reverse osmosis (RO) and nanofiltration (NF) for the reclamation of ultra-filtered treated sewage effluent (TSE) for irrigation of food crops. RO and NF technologies were evaluated at different applied pressures, the performance of each technology was evaluated in terms of water flux, recovery rate, specific energy consumption and quality of permeate. It was found that the permeate from the reverse osmosis (RO) process complied with the Food and Agriculture Organization (FAO) standards at applied pressures between 10 bar and 18 bar. At an applied pressure of 20 bar the permeate quality did not comply with irrigation water standards in terms of chloride, sodium and calcium concentration. It was found that the nanofiltration process was not suitable for the reclamation of wastewater as the concentration of chloride, sodium and calcium exceeded the allowable limits at all applied pressures. In the reverse osmosis process, the highest recovery rate was 36% achieved at an applied pressure of 16 bar. The specific energy consumption at this applied pressure was 0.56 kWh/m^3. The lowest specific energy of 0.46 kWh/m^3 was achieved at an applied pressure of 12 bar with a water recovery rate of 32.7%.

Keywords: Irrigation water; Reverse osmosis; Nanofiltration; Treated sewage effluent; Water reuse.

1. Introduction

Water scarcity is one of the most challenging problems that affect agriculture worldwide, especially in arid areas. The united nations estimates that agriculture accounts for 70% of water usage around the world (Hafiz et al., 2019). Treated wastewater is an economical solution to be used as irrigation water and a source of nutrients (Shanmuganathan et al., 2015). Treated wastewater can improve soil health and reduce fertilizers consumption. However, treated wastewater may also damage the soil because of the excess salts, pathogens, organics, sodium, and chloride content. The water quality for irrigation water is mainly characterized in terms of total dissolved salts, pH, and different ions and cations concentration (e.g. Na, Cl, NO_3, SO_4, PO_4, K, Ca, and Mg). Enhancing the quality of treated wastewater to meet irrigation standards has become a must practice. In order to reach the required quality of treated wastewater membrane technologies are considered to be a critical element.

(Shanmuganathan et al., 2015) studied the possibility of enhancing the quality of micro-filtered treated sewage effluent using nanofiltration (NF) and reverse osmosis (RO). The study showed that using NF and RO alone could not produce permeate, which meets irrigation standards. Irrigation suitable permeate was produced using an NF-RO hybrid system. Also, it was found that utilizing NF before RO reduced the RO membrane fouling. (Li et al., 2016) studied the performance of advanced treatment of municipal wastewater by nanofiltration. The study evaluated the effect of operating pressure and feed solution pH. The experimental results showed that optimum performance was achieved using a 12 bar pressure, pH = 4 and a flow rate of 8 LPM. Protein-like substances of high molecular weight (MW) are the dominant foulants on the membrane surface. A pilot-scale study conducted by Oron et al. (2006) showed that by using a hybrid ultrafiltration- reverse osmosis (UF-RO) technology, water suitable for irrigation could be produced from secondary treated municipal wastewater (Oron et al., 2006). The cost of the process was between 0.16 and 0.24 US$/$m^3$ water. Mrayed et al. (2011) applied a hybrid nanofiltration-reverse osmosis (NF-RO) system to produce irrigation water from secondary treated effluent. They used polyacrylic acid (PAA) as a chelating agent. The addition of PAA helped in the formation of covalent bonds among different nutrients in the feed, which improved the rejection rate for those nutrients. (Egea-Corbacho et al., 2019) tested the performance of a pilot-scale nanofiltration membrane for the treatment of secondary treated wastewater effluent. It was found that the product water quality complies with Spanish Royal Decree 1620/2007. This was concluded by considering E Coli, TSS and turbidity, but the authors did not compare the concentration of various elements in the permeate water with allowable limits (i.e. phosphates, nitrates, total dissolved solids, ammonium, sodium and chloride). A study from (Chon et al., 2012) used a hybrid technology comprising of membrane bioreactor and nanofiltration to produce irrigation water from municipal wastewater. It was found that the physicochemical properties and molecular weight cut off were the most critical aspect in the removal of nutrients from the water. (Gu et al., 2019) evaluated the performance of trihybrid anaerobic membrane bioreactor (AnMBR)-reverse osmosis (RO)-ion exchange (IE) process for reclamation of microfiltered municipal wastewater to high-grade clean water. The net energy consumption of the process was 1.16 kWh/$m^{3,}$ and product water was found to be suitable for industrial and indirect potable applications. Hafiz et al. (2019) used FO to produce irrigation water from treated sewage effluent (TSE). The feed solution and draw solution for the FO was TSE and an engineered fertilizing solution (0.5 M NaCl & 0.01 M $(NH_4)_2HPO_4$), respectively. The draw solution was regenerated using RO. The specific power consumption was between 2.18 and 2.58 kWh/m^3. (Liu et al., 2011) evaluated the effectiveness of nanofiltration and reverse osmosis in the treatment of treated textile effluent in terms of salinity reduction and COD rejection. The results showed that nanofiltration exhibited more severe flux decline compared to reverse osmosis (RO) because of the higher porosity and membrane fouling of the nanofiltration membrane. RO showed higher total salts rejection compared to NF. (Qi et al., 2020) analyzed pollutants removal efficiency and operating costs of municipal wastewater treatment plants in china. Significant difference in removal efficiencies was observed among various pollutants, with the highest removal efficiency in BOD_5 and lowest removal efficiency in TN. Higher nitrogen removal should be achieved to obtain the desired water quality outcomes.

So far, previous studies evaluated the performance of various membrane processes for the reclamation of secondary treated sewage effluent. Little information is available for the performance of the nanofiltration and the reverse osmosis membranes in the generation of irrigation water from tertiary treated wastewater. It is recommended to select a single membrane process that can generate high-quality irrigation water from treated sewage effluent at minimal energy requirement. The product water quality must comply with the Food and Agriculture Organization (FAO) standards.

The objective of this paper is to evaluate the efficiency of nanofiltration and reverse osmosis to treat ultra-filtered tertiary treated sewage effluent (TSE) for the product water to be used in irrigation for food crops. The performance of each technology was evaluated under different applied pressures in terms of water flux, recovery rate, energy consumption and quality of permeate.

2. Materials and setup

2.1 Feedwater

Ultra-filtered tertiary treated sewage effluent (TSE) was used as feedwater to the nanofiltration and reverse osmosis processes. TSE was collected from a wastewater treatment plant located in Doha, Qatar. The wastewater treatment plant consists of preliminary, secondary and tertiary treatment processes. The tertiary treatment process consists of a multimedia filter followed by ultrafiltration and UV disinfection. The characteristics of the collected, treated sewage effluent are summarized in Table 1. The max limit of the listed parameters was recommended by FAO (Ayres and Westcot, 1985; Lejalem et al., 2018; Parlar et al., 2019). The use of this feed water on food crops was unsuitable because of excessive TDS and high ions-cations. The concentration of heavy metals was below the maximum limit recommended by FAO. The conductivity of samples was measured using OAKTON PCD650 multi-meter. Anions concentration was measured by ion chromatography (Metrohm 850 Professional IC), and cations concentration was measured using plasma emission spectroscopy (iCAP 6500-ICP-OES CID) (Thermo Scientific). Before measuring the concentration of anions and cations, samples with a conductivity value above 1 mS/cm were diluted using deionized water to a conductivity value below 1 mS/cm. This is done to eliminate the interference of high peaks of Na and Cl, which may affect the readings of other elements. The turbidity was measured using a turbidity meter (Hach 2100p). Metal concentration was measured using ICP-MS (Nexion 300D).

Table 1. Characteristics of tertiary treated sewage effluent (feed water)

Parameter	Value	Max Limit	Standard Method
TDS (ppm)	1461 ± 5	750	APHA 2540 C. Total Dissolved Solids Dried at 180 °C
Turbidity (NTU)	0.2 ± 0.1	2	APHA 2130 B. Nephelometric Method
EC (mS/cm)	2.56 ± 0.2	0.7	APHA 2510 B. Conductivity
Fluoride (ppm)	0.27 ± 0.2	1.5	APHA 4110 Determination of anions by ion chromatography
Chloride (ppm)	897.5 ± 0.2	106.5	
Bromide (ppm)	0.96 ± 0.2	1	
Nitrate (ppm)	25.84 ± 0.2	20	
Sulfate (ppm)	320.3 ± 0.2	400	

Sodium (ppm)	200.3 ± 0.2	69	APHA 3120 Determination of metals by plasma emission spectroscopy
Potassium (ppm)	12.4 ± 0.2	10	
Calcium (ppm)	87.7 ± 0.2	40	
Magnesium (ppm)	21.4 ± 0.2	24	
Boron (ppb)	158.97 ± 0.1	500	EPA Method 200.8
Vanadium (ppb)	0.11 ± 0.1	100	
Manganese (ppb)	11.54 ± 0.1	200	
Cobalt (ppb)	0.17 ± 0.1	50	
Nickel (ppb)	23.11 ± 0.1	200	
Copper (ppb)	13.08 ± 0.1	200	
Zinc (ppb)	151.58 ± 0.1	2000	
Cadmium (ppb)	0.2 ± 0.1	10	
Beryllium (ppb)	2.02 ± 0.1	100	

2.2 Experimental setup

A schematic sketch for the bench-scale membrane testing skid is shown in Fig.1. A crossflow CF042D cell made of natural acetal copolymer (Delrin) provided by Sterlitech was used in the nanofiltration and reverse osmosis processes. The cell dimensions are 12.7 x 8.3 x 10 cm with active inner dimensions of 4.6 x 9.2 cm and 0.23 cm slot depth. Two tanks were used to store the feed and the permeate water. A M-03S HYDRACELL pump (230V, 50HZ, 3PH, 6.7 LPM) was used to pressurize the feed solution through the membrane. A water chiller (PolyScience Chiller) was used to maintain the feedwater temperature at room temperature (25 ± 2 °C). A concentrate/back pressure control valve was used to control the water flow through the system and to regulate pressure in the system. Flow meters (Sterlitech Read Panel Mount Flow Meter) were used to measure the flow rate at specific points in the system. A digital balance (Mettler Toledo – ICS 241) was connected to a computer to measure the permeate flux in the system. A specific quantity (3 L) of tertiary treated sewage effluent (TSE) was used as a feed solution in both processes. The applied pressure in the RO and the NF processes varied between 10 bar and 20 bar with an increase of 2 bar for each experiment. The flow rate was 3.5 LPM and the experimental running time was 4 h. The used RO membrane was BW30LE produced by DOW FILMTEC. The used RO membrane is a polyamide – TFC membrane with a pore size of 100 Da. The used NF membrane was NF90 produced by DOW FILMTEC. The used NF membrane is a polyamide – TFC membrane with a pore size of 200-400 Da.

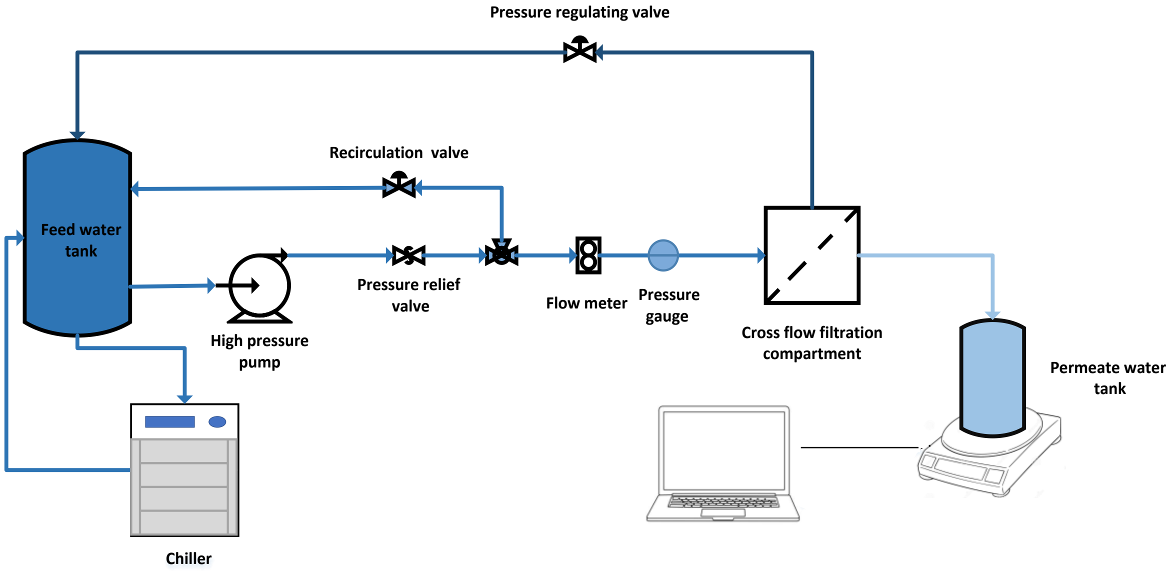

Figure 1. Schematic diagram of cross flow lab scale membrane test skid

2.3 Error estimation

All experiments were performed in triplicates and the reported results are the average of the three experimental trials. The error bars represent the standard deviation of each reading.

3. Results and Discussion

3.1 Effect of feed pressure on water flux and recovery rate

The water flux (J_w) in the RO process and the NF process was calculated using Eq.1 (Thabit et al., 2019):

$$J_w = \left(\frac{V_p}{A_m \times t}\right) \quad (1)$$

Here, V_P is the volume of the permeate (L), A_m is the area of the membrane (m^2), t is the operating time (h). Figure 2 (a) and (b) shows the change of water flux with time in the RO and NF process, respectively. It can be seen from Fig.2 (a) and (b) that the water flux decreased with time at all applied pressures. The decrease in the water flux with time is due to the concentration of the feed solution where the reject solution was recycled back into the system and membrane fouling. TSE contains traces of organic matter, which could accumulate on the surface of the membrane and cause fouling (Ortega-Bravo et al., 2016). It can also be seen from Fig.2 (a) that in the RO process the water flux at an applied pressure of 12 – 20 bar was within the same range, but at an applied pressure of 10 bar the water flux was much lower. In the NF process, the water flux at an applied pressure of 12 bar was higher than the water flux at the other applied pressures. This was done to compare the performance of the RO and the NF processes at the different applied pressures; the average water flux was calculated.

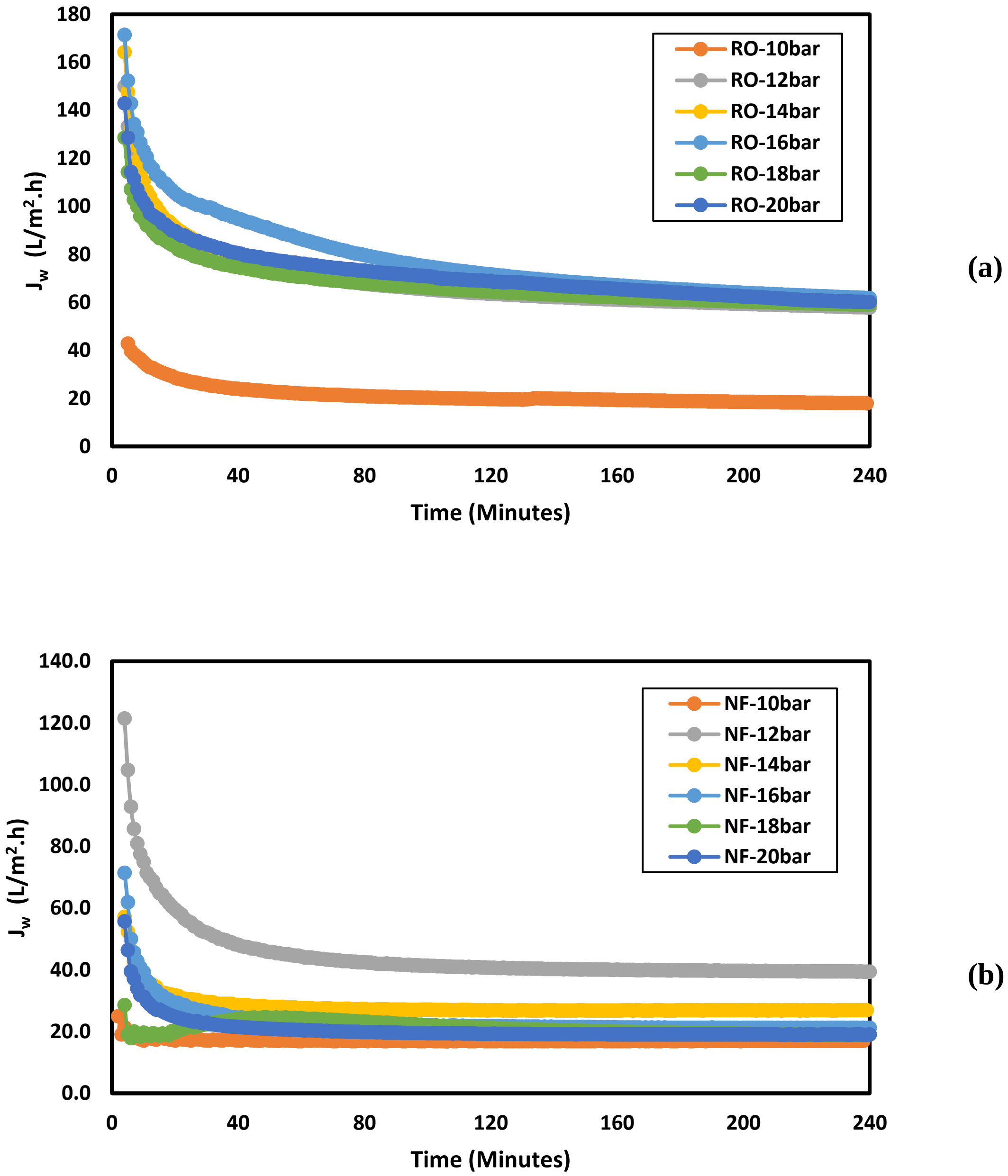

Figure 2. Water flux using TSE as feed water at different applied pressure in (a) Reverse osmosis (b)Nanofiltration

Figure 3 shows the average water flux for RO and NF at different feed pressures. In RO, when the applied pressure was 10 bar the average water flux was 21.3 L/m^2.h. When the applied pressure increased to 12 bar the average water flux increased by 69%, to reach a value of 68.1 L/m^2.h. At a 14 bar applied pressure, the average water flux further increased to reach a value of 71.5 L/m^2.h. At an applied pressure of 16 bar the average water flux reached a maximum value of 77.7 L/m^2.h. As the applied pressure further increased the average water flux decreased. Where at an applied pressure of 18 bar and 20 bar the average water flux was 71.6 L/m^2.h and 67.5 L/m^2.h, respectively. A different trend was observed in the NF process. Excluding the 10 bar applied pressure experiment, it was found that the average water flux decreased as the applied pressure increased (Fig.3). The maximum average water flux was 44.5 L/m^2.h obtained at an applied pressure of 12 bar. When the applied pressure increased to 14 bar the average water flux decreased by almost 37% to reach a value of 28.1 L/m^2.h. As the applied pressure further increased the average water flux kept decreasing to reach a minimum value of 20.6 L/m^2.h at an applied pressure of 20 bar. The water permeability is expected to increase as the feed pressure increases; however, applying excessive pressure may result in excessive accumulation of foulants on the surface of the membrane which may result in lower average water flux (Jiang et al., 2017). The average water flux of RO was higher than NF. In effect, the NF membrane is prone to fouling compared to RO membrane, because the nanofiltration membrane has a rougher, thicker and hydrophobic surface when compared to the reverse osmosis membrane (Xu et al., 2010). The lowest average water flux for RO and NF was obtained at an applied pressure of 10 bar. The water diffusion through the membrane starts to occur when the applied pressure exceeds the natural osmotic pressure of the solution. The osmotic pressure of the feed solution was almost 9 bar; consequently, a feed pressure of 10 bar was not enough to acquire high water flux.

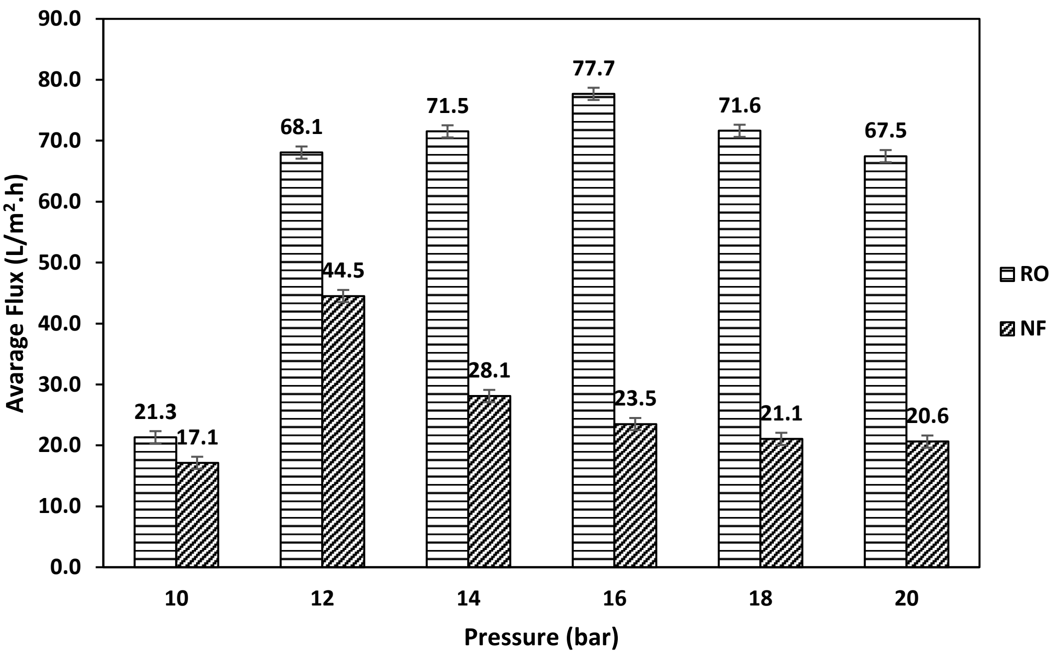

Figure 3. Average water flux of RO and NF at different feed pressure

The recovery rate ($R\%$) has been calculated using Eq.2 (Singh et al., 2019):

$$\%R = \left(\frac{V_P}{V_F}\right) \times 100\% \tag{2}$$

Here, V_P and V_F are the volume of the permeate and the feed solution, respectively. Figure 4 shows the recovery rate for RO and NF at different feed pressures. In the RO process, the highest water recovery was 36% obtained at an applied pressure of 16 bar. The lowest water recovery was 10.2% obtained at an applied pressure of 10 bar. When the applied pressure was 12 bar, the water recovery was 32.7% which is 3.3% lower than the maximum water recovery obtained at 16 bar feed pressure. When the applied pressure was 14 bar, the water recovery was 35.2% which is only 0.8% lower than the maximum water recovery obtained at 16 bar feed pressure. As the feed pressure increased more than 16 bar, the water recovery decreased. At a feed pressure of 18 bar the water recovery was 34.3%, and at a feed pressure of 20 bar the water recovery was 33.8%. As mentioned earlier, applying excessive pressure may result in the accumulation of foulants on the membrane surface, which could result in lower water production (Qasim et al., 2019). In nanofiltration, the maximum recovery rate was 21.9% obtained at a feed pressure of 12 bar. The recovery rate decreased dramatically from 21.9% to 14.9% at an applied pressure of 14 bar. As the pressure increased, the recovery rate decreased to reach a value of 10.6% at an applied pressure of 20 bar. The recovery rate of nanofiltration was found to be lower than reverse osmosis. In addition, the effect of pressure is more apparent in nanofiltration. The NF membrane has a higher negative charge compared to the RO membrane, which makes the NF membrane more prone to fouling (Zou et al., 2018). In addition, the nanofiltration membrane has a rougher, thicker and less hydrophilic surface when compared to the reverse osmosis membrane (Chen et al., 2017). The used nanofiltration membrane (NF 90) had a contact angle of 67.5^{o} while the used reverse osmosis membrane (BW30LE) had a contact angle 33° (Gryta et al., 2012). This could have also caused the lower recovery rates obtained by NF compared to RO.

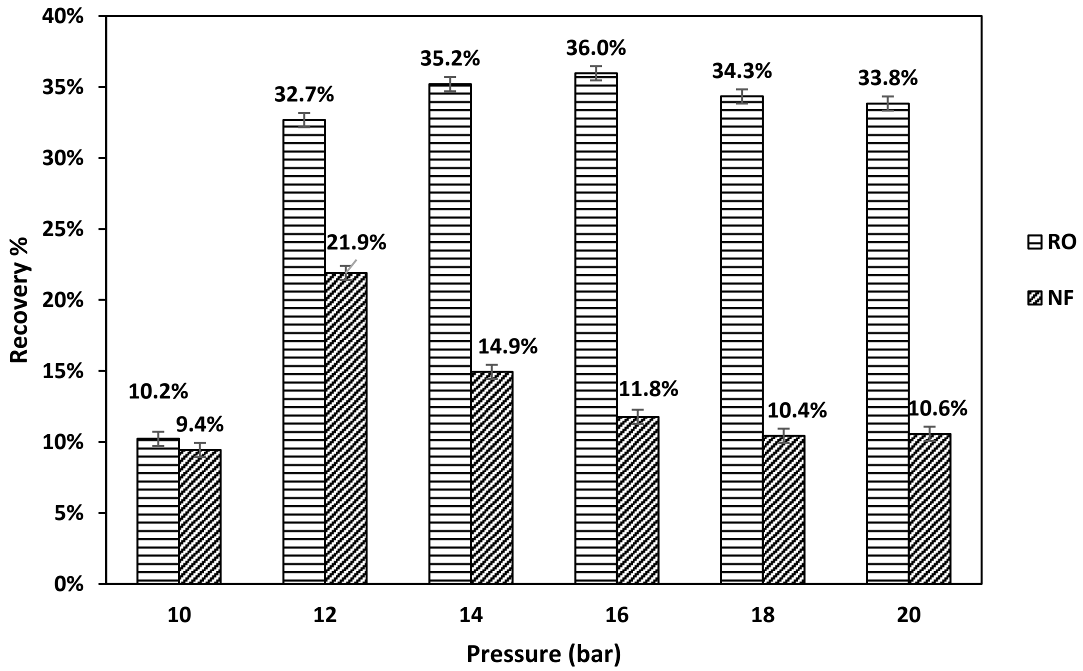

Figure 4. Recovery rate of RO and NF at different feed pressure

SEM images of unused and used RO and NF membranes at different applied pressures are shown in Fig.5. Fig. 5 (b), (c) and (d) show the used RO membranes at an applied pressure of 12, 16 and 20 bar, respectively. It can be seen from the SEM images that as the applied pressure increased more accumulation of foulant materials occurred on the surface of the membrane. A similar observation was detected on the nanofiltration membrane where the amount of the accumulated foulants increased on the surface of the membrane as the feed pressure increased (Fig.5 (f), (g) and (h)). From the EDX analysis shown in Table 2, it can be seen that after the use of the RO and NF membranes new elements were detected on the surface of the membranes such as sulfur, iron, and phosphorus, which also indicates the accumulation of foulant materials on the surface of the membrane. The accumulation of these elements on the surface of the membrane negatively affected the water flux. The accumulation of metal ions on the surface of the membrane may further tie the fouling materials on the membrane material resulting in enhanced compactness of the fouling layer (Sun et al., 2019).

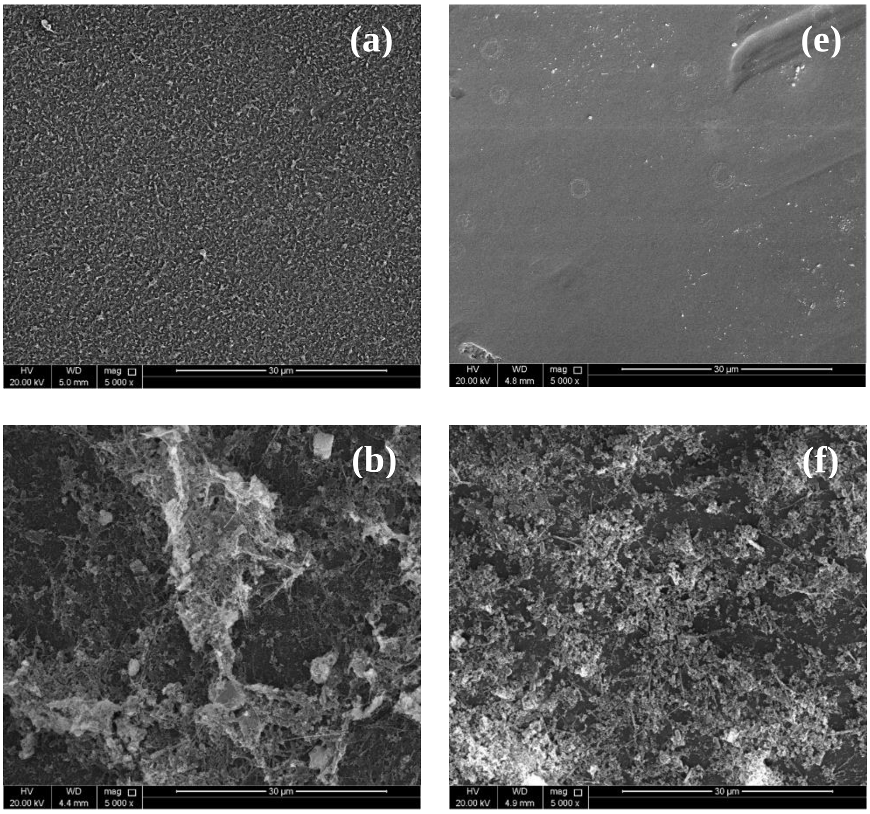

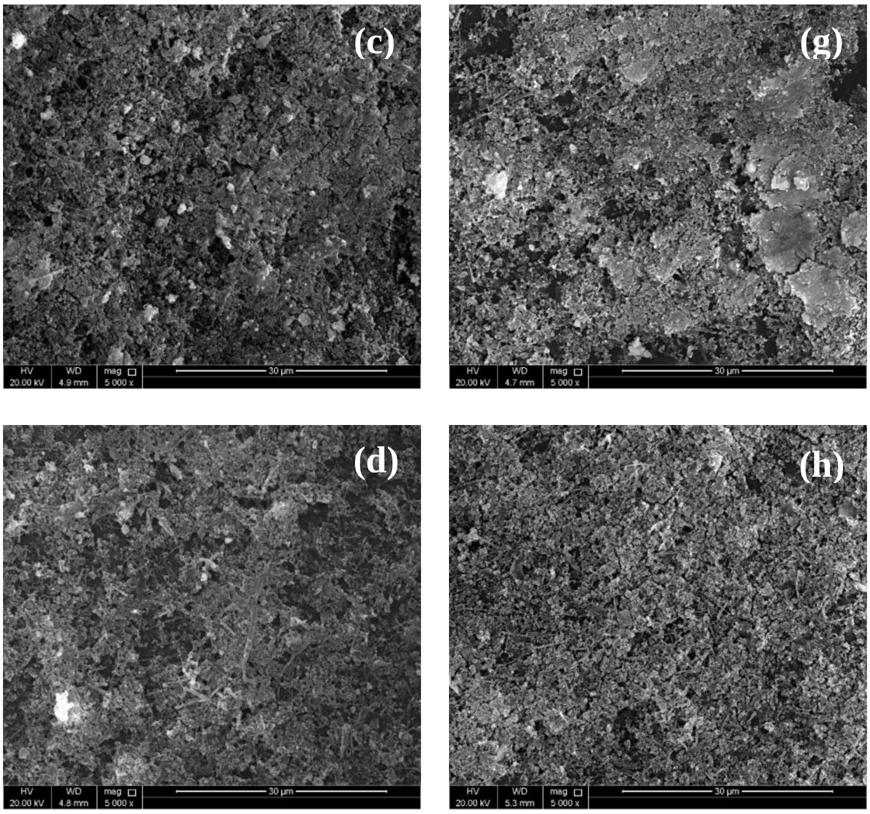

Figure 5. SEM images of (a) Clean RO membrane, (b) Tested RO membrane at a feed pressure of 12 bar, (c) Tested RO membrane at a feed pressure of 16 bar, (d) Tested RO membrane at a feed pressure of 20 bar, (e) Clean NF membrane, (f) Tested NF membrane at a feed pressure of 12 bar, (g) Tested NF membrane at a feed pressure of 16 bar, (h) Tested NF membrane at a feed pressure of 20 bar.

Table 2. EDX analysis of elements wt% on the surface of a clean and tested RO and NF membranes

Membrane	**Weight %**					
	[C]	**[O]**	**[S]**	**[Fe]**	**[P]**	**[Other]**
RO-clean	87.39	9.53	3.08	0	0	0
RO-tested	70.64	19.45	3.32	1.79	0.66	4.14
NF-clean	89.78	6.66	3.56	0	0	0
NF- tested	73.96	16.32	3.94	1.91	0.48	3.39

3.3 Energy consumption

The specific energy consumption (E_s) of the RO and the NF processes has been calculated using Eq.3 (Shrivastava and Stevens, 2018):

$$E_s = \left(\frac{P}{n \times \%R}\right) \quad (3)$$

Here, P is the applied feed pressure (bar), *n* is the pump efficiency, %R is the recovery rate. The specific energy consumption depends on the applied pressure and the recovery rate; therefore, the lowest energy consumption will be obtained at a high recovery rate using low applied pressure. Figure 6 shows the specific energy consumption of the RO process and the NF process at different feed pressures. In the NF process, the specific energy consumption increased from 0.68 kWh/m^3 to 2.35 kWh/m^3 at a feed pressure of 12 bar and 20 bar, respectively. As shown in Eq.3, the specific energy is a function of applied pressure and recovery rate. At a low feed pressure of 10 bar the specific energy consumption was 1.33 kWh/m^3. The high specific energy consumption at such low feed pressure is due to the low recovery rate obtained at 10 bar feed pressure (Fig.4). The maximum energy consumption was 2.35 kWh/m^3, which was obtained at a feed pressure of 20 bar. The high specific energy consumption at such high applied pressure is due to the low recovery (Fig.4). In the RO process, the same trend was observed where the specific energy consumption increased from 0.46 kWh/m^3 to 0.73 kWh/m^3 at a feed pressure of 12 bar and 20 bar, respectively. At a low feed pressure of 10 bar the specific energy consumption was 1.22 kWh/m^3, which is due to the low recovery rate obtained at such low applied pressure as shown in Fig.4. It was found that the NF process at an applied pressure of 12 bar gave the highest water recovery rate and the lowest energy consumption. For the RO process, the lowest energy consumption was found at an applied pressure of 12 bar while the highest water recovery rate was at an applied pressure of 16 bar. The difference in the water recovery rate between the 12 and 16 bar applied pressure in the RO process was only 3.3%. In comparison, the energy consumption was 18% higher at an applied pressure of 16 bar when compared to 12 bar applied pressure. The quality of the produced permeate should be analyzed to investigate which process and which running conditions to be utilized.

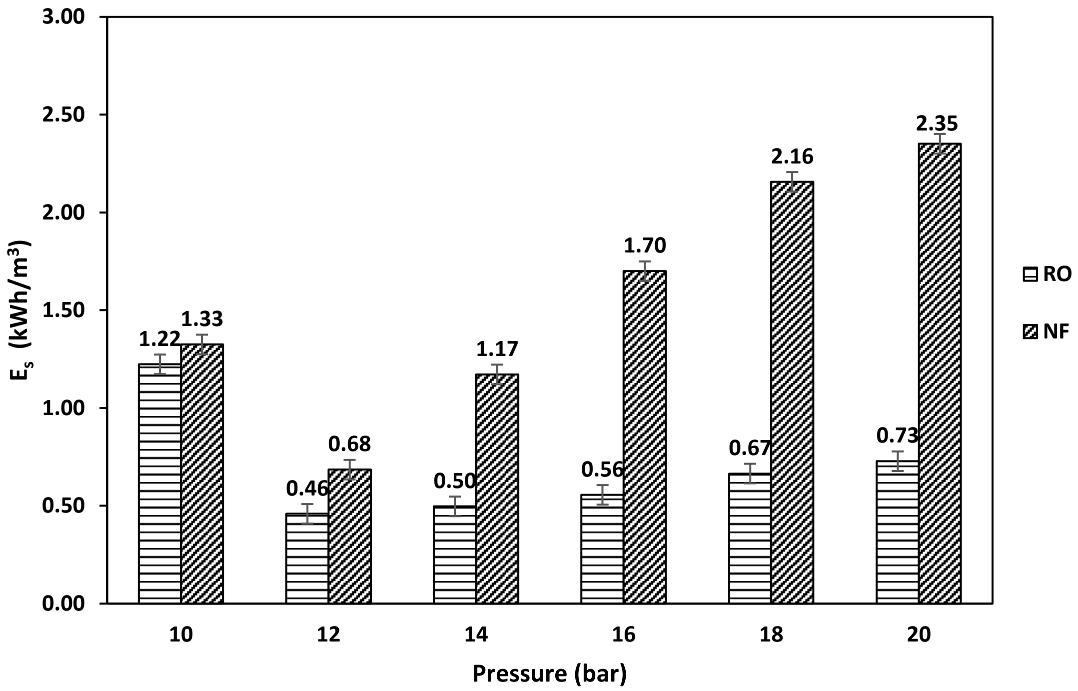

Figure 6. Specific energy consumption of RO and NF at different feed pressure.

3.4 Product water quality

Characteristics of the produced permeate were measured for the RO and the NF processes. The quality of the produced permeate was compared with the Food and Agriculture Organization (FAO) standards (Ayres and Westcot, 1985). As shown in Fig.7 (a) the concentration of the different measured elements in the produced permeate from the RO process at applied pressures between 10 and 18 bar was within the FAO standards. At an applied pressure of 20 bar, multiple parameters such as TDS, conductivity, chloride, sodium and calcium concentration exceeded the allowable limits. In the NF process (Fig.7 (b)), under all applied pressures, the permeate quality did not comply with FAO standards. It was noticed that the elements that did not comply with the standards were chloride, sodium and calcium. The high concentration of these elements in return affected the TDS concentration. For example, at 12 bar applied pressure where the highest water recovery rate was attained the TDS concentration was almost 21% higher than the allowable limit, and the chloride, sodium and calcium concentrations were 84%, 61% and 13% higher than the allowable limit, respectively. It could be noticed that the NF membrane had a low rejection rate for monovalent ions, where the rejection rate for chloride and sodium was only 27% and 12%, respectively.

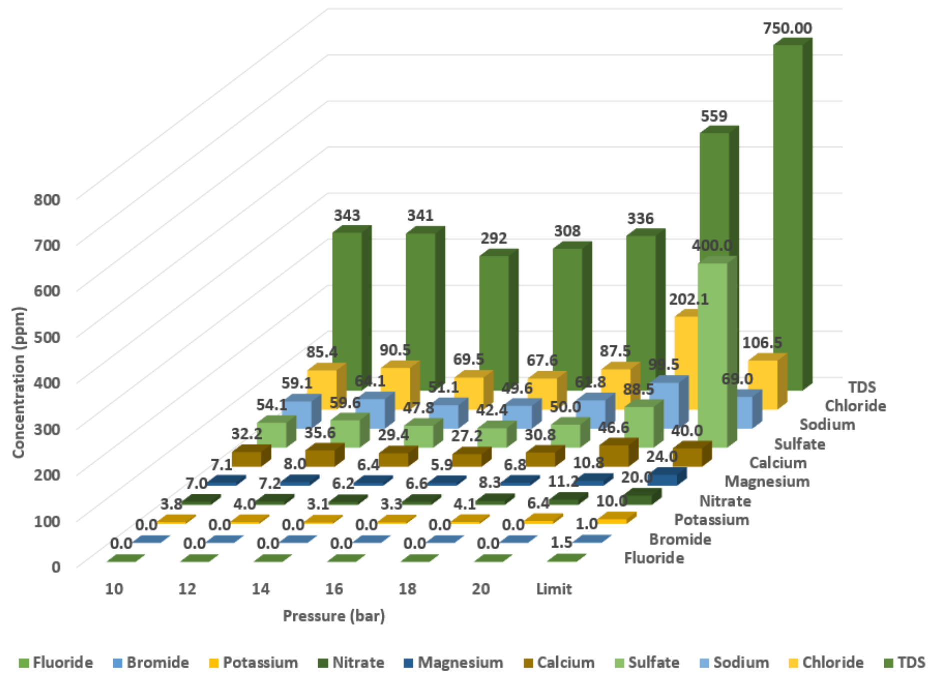

(a)

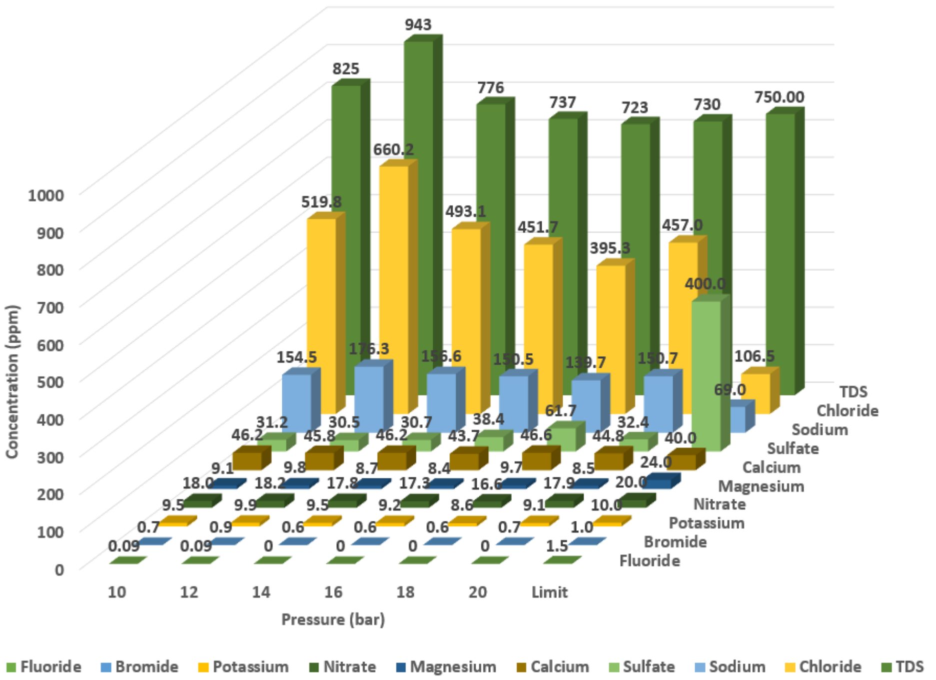

(b)

Figure 7. Characteristics of the permeate produced from treated sewage effluent (TSE) using (a) Reverse osmosis (b)Nanofiltration at different applied pressures.

It can be inferred that using a single-stage NF is not possible due to low water quality, and it is recommended to use RO at applied pressure between 10 and 18 bar. Selecting the most suitable applied pressure to operate the RO process depends on water flux, recovery rate, energy consumption and product water quality. It was found in the previous sections that the lowest energy consumption of RO was obtained at an applied pressure of 12 and 14 bar. After considering the water quality, it is recommended to use an applied pressure of 14 bar due to higher water quality.

4. Conclusions

In this paper, a comparative study was done on the reclamation of tertiary treated sewage effluent (TSE) by nanofiltration and reverse osmosis for water reuse in irrigation. The results reported show that reverse osmosis (RO) is capable of reclaiming tertiary treated sewage effluent (TSE) to be used as irrigation water for food crops. NF is not suitable for the reclamation of wastewater because of the low rejection of monovalent ions. In nano-filtered TSE, the concentration of Na and Cl exceeded the maximum allowable limits recommended by FAO. RO is suitable for the reclamation of wastewater due to high water quality and water flux. In the RO process, the highest recovery rate was 36% achieved at an applied pressure of 16 bar. The specific energy consumption at this applied pressure was 0.56 kWh/m^3. At 14 bar applied pressure, the recovery rate was only 2% lower than that at an applied pressure of 16 bar, while the specific energy consumption was almost 11% lower. At 12 bar applied pressure, the specific energy consumption was 8% higher than the specific energy at an applied pressure of 14 bar while the recovery rate was 7% higher. It is recommended to use RO process at 14 bar applied pressure for the reclamation of TSE. This is due to the high recovery rate, low energy consumption and high water quality compared to other available technologies. The product water could meet the quality requirements of the Food and Agriculture Organization (FAO). The results from this study might lead to a paradigm shift in the reclamation of tertiary treated wastewater to be used for the irrigation of food crops.

Declaration of competing interest

The authors declare that they have no known competing financial interests or personal relationships that could have appeared to influence the work reported in this paper.

CRediT authorship contribution statement

MhdAmmar Hafiz: Conceptualization, Data collection, Data analysis, Writing manuscript. **Alaa H. Hawari**: Conceptualization, Methodology, Review & editing. **Radwan Alfahel**: Data collection, Data analysis. **Ali altaee**: Conceptualization, Methodology, Review & editing.

Acknowledgements

This research is made possible by graduate sponsorship research award (GSRA6-1-0509-19021) from Qatar National Research Fund (QNRF). The statements made herein are solely the responsibility of the authors. We would also like to thank Central Laboratories Unit (CLU) at Qatar University for generating SEM images and the ion chromatography tests.

References

Ayres, R.S., Westcot, D.W., 1985. FAO IRRIGATION AND DRAINAGE PAPER. Food and Agriculture Organization of the United Nations.

Chen, Z., Luo, J., Hang, X., Yinhua, W., 2017. Physicochemical characterization of tight nanofiltration membranes for dairy wastewater treatment. Journal of Membrane Science 547.

Chon, K., KyongShon, H., Cho, J., 2012. Membrane bioreactor and nanofiltration hybrid system for reclamation of municipal wastewater: Removal of nutrients, organic matter and micropollutants. Bioresource Technology 122, 181-188.

Egea-Corbacho, A., Gutiérrez Ruiz, S., Quiroga Alonso, J.M., 2019. Removal of emerging contaminants from wastewater using nanofiltration for its subsequent reuse: Full–scale pilot plant. Journal of Cleaner Production 214, 514-523.

Gryta, M., Bastrzyk, J., Lech, D., 2012. Evaluation of fouling potential of nanofiltration membranes based on the dynamic contact angle measurements. Polish Journal of Chemical Technology 14.

Gu, J., Liu, H., Wang, S., Zhang, M., Liu, Y., 2019. An innovative anaerobic MBR-reverse osmosis-ion exchange process for energy-efficient reclamation of municipal wastewater to NEWater-like product water. Journal of Cleaner Production 230, 1287-1293.

Hafiz, M.A., Hawari, A.H., Altaee, A., 2019. A hybrid forward osmosis/reverse osmosis process for the supply of fertilizing solution from treated wastewater. Journal of Water Process Engineering 32, 100975.

Jiang, S., Li, Y., Ladewig, B.P., 2017. A review of reverse osmosis membrane fouling and control strategies. Science of The Total Environment 595, 567-583.

Lejalem, A., Dagnaw, Chandravanshi, B., Zewge, F., Ababa, A., 2018. Fluoride content of leafy vegetables, irrigation water, and farmland soil in the rift valley and in non-rift valley areas of Ethiopia. Fluoride 50.

Li, K., Wang, J., Liu, J., Wei, Y., Chen, M., 2016. Advanced treatment of municipal wastewater by nanofiltration: Operational optimization and membrane fouling analysis. Journal of Environmental Sciences 43, 106-117.

Liu, M., Lü, Z., Chen, Z., Yu, S., Gao, C., 2011. Comparison of reverse osmosis and nanofiltration membranes in the treatment of biologically treated textile effluent for water reuse. Desalination 281, 372-378.

Mrayed, S.M., Sanciolo, P., Zou, L., Leslie, G., 2011. An alternative membrane treatment process to produce low-salt and high-nutrient recycled water suitable for irrigation purposes. Desalination 274(1), 144-149.

Oron, G., Gillerman, L., Bick, A., Buriakovsky, N., Manor, Y., Ben-Yitshak, E., Katz, L., Hagin, J., 2006. A two stage membrane treatment of secondary effluent for unrestricted reuse and sustainable agricultural production. Desalination 187(1), 335-345.

Ortega-Bravo, J.C., Ruiz-Filippi, G., Donoso-Bravo, A., Reyes-Caniupán, I.E., Jeison, D., 2016. Forward osmosis: Evaluation thin-film-composite membrane for municipal sewage concentration. Chemical Engineering Journal 306, 531-537.

Parlar, I., Hacıfazlıoğlu, M., Kabay, N., Pek, T.Ö., Yüksel, M., 2019. Performance comparison of reverse osmosis (RO) with integrated nanofiltration (NF) and reverse osmosis process for desalination of MBR effluent. Journal of Water Process Engineering 29, 100640.
Qasim, M., Badrelzaman, M., Darwish, N.N., Darwish, N.A., Hilal, N., 2019. Reverse osmosis desalination: A state-of-the-art review. Desalination 459, 59-104.
Qi, M., Yang, Y., Zhang, X., Zhang, X., Wang, M., Zhang, W., Lu, X., Tong, Y., 2020. Pollution reduction and operating cost analysis of municipal wastewater treatment in China and implication for future wastewater management. Journal of Cleaner Production 253, 120003.
Shanmuganathan, S., Vigneswaran, S., Nguyen, T.V., Loganathan, P., Kandasamy, J., 2015. Use of nanofiltration and reverse osmosis in reclaiming micro-filtered biologically treated sewage effluent for irrigation. Desalination 364, 119-125.
Shrivastava, A., Stevens, D., 2018. Chapter 2 - Energy Efficiency of Reverse Osmosis, in: Gude, V.G. (Ed.) Sustainable Desalination Handbook. Butterworth-Heinemann, pp. 25-54.
Singh, N., Dhiman, S., Basu, S., Balakrishnan, M., Petrinic, I., Helix-Nielsen, C., 2019. Dewatering of sewage for nutrients and water recovery by Forward Osmosis (FO) using divalent draw solution. Journal of Water Process Engineering 31, 100853.
Sun, F., Lu, D., Ho, J.S., Chong, T.H., Zhou, Y., 2019. Mitigation of membrane fouling in a seawater-driven forward osmosis system for waste activated sludge thickening. Journal of Cleaner Production 241, 118373.
Thabit, M.S., Hawari, A.H., Ammar, M.H., Zaidi, S., Zaragoza, G., Altaee, A., 2019. Evaluation of forward osmosis as a pretreatment process for multi stage flash seawater desalination. Desalination 461, 22-29.
Xu, P., Bellona, C., Drewes, J.E., 2010. Fouling of nanofiltration and reverse osmosis membranes during municipal wastewater reclamation: Membrane autopsy results from pilot-scale investigations. Journal of Membrane Science 353(1), 111-121.
Zou, L., Zhang, S., Liu, J., Cao, Y., Qian, G., Li, Y.-Y., Xu, Z.P., 2018. Nitrate removal from groundwater using negatively charged nanofiltration membrane. Environmental Science and Pollution Research.